

## Fractal nature of porous silicon nanocrystallites

T. Nychyporuk, V. Lysenko, and D. Barbier

Materials Physics Laboratory (LPM), CNRS UMR-5511, INSA de Lyon, 7 Avenue Jean Capelle, Bâtiment Blaise Pascal, 69621 Villeurbanne Cedex, France

(Received 8 May 2004; revised manuscript received 5 January 2005; published 1 March 2005)

Experimental study of the hydrogen coverage of a nanoporous silicon-specific surface reveals a fractal nature of the surface of silicon nanocrystallites constituting the porous layer. A fractal model describing the nanocrystallite morphology is elaborated. The evolution of the nanocrystallites' fractal dimension (2.1–2.4) along with porosity is deduced from a correlation of the model to the experimental measurements of hydrogen concentration.

DOI: 10.1103/PhysRevB.71.115402

PACS number(s): 68.65.-k, 61.46.+w, 61.43.Hv, 61.43.Gt

### I. INTRODUCTION

Porous materials are frequently encountered examples of naturally disordered media. Porous silicon (PS) nanostructures and their physical properties were also objects of numerous attempts to be described by fractal models.<sup>1,2</sup> From a comparison of electron microscopy data with computer models,<sup>3</sup> from small-angle x-ray<sup>4,5</sup> and neutron<sup>6</sup> scattering as well as from atomic force microscopy observations,<sup>7,8</sup> it is known that the PS network has a fractal structure. A fractal model of pore formation in a PS layer was recently proposed<sup>9</sup> by Aroutiounian *et al.* The fractal structure of PS was found to govern its ac conductivity in a low-frequency regime<sup>10</sup> and was recently supported by Raman and photoluminescence spectroscopies.<sup>11</sup> Being relatively well described at a macroscopic scale (i.e., at the level of the whole PS network), the porosity dependence of the fractal nature of the nanocrystallites forming the PS structure was never, to our knowledge, brought to the fore, while the fractal nature of the nanocrystallites constituting PS layers was already quantitatively treated in one of our recent papers.<sup>12</sup> Now, in this paper we present (i) experimental results reflecting clearly a porosity-dependent fractal nature of the specific-surface of the silicon nanocrystallites constituting the PS nanostructure, (ii) a fractal model describing the specific-surface nanostructuring, and finally, (iii) the porosity dependence of the specific-surface fractal dimensions obtained from a comparison of the experimental results and the elaborated model.

### II. EXPERIMENTAL METHODS

#### A. Porous silicon formation and structural characterization

Our PS samples were produced according to a standard procedure<sup>13</sup> of electrochemical etching of monocrystalline (100)-oriented boron-doped (1–10  $\Omega$  cm) Si wafers at current densities, 2–300 mA cm<sup>2</sup>. The etching solutions were 9:1 and 3:1 (by volume) mixtures of concentrated aqueous hydrofluoric acid (48%) and ethanol.

Depending on the current density and on the etching solution composition, the porosity of the layers (40–90 %) was estimated from the PS refractive index measurements performed by means of a Perkin-Elmer GSX-2 Fourier transformation infrared (FTIR) spectrometer used in reflective back-

scattering geometry and from the correlation of the index values to porosity by using Bruggeman's effective media model.<sup>14</sup> The PS refractive indexes were deduced from the spectral position of the interferential fingers detected in the 3000–5000 cm<sup>-1</sup> spectral range for the optically thin PS samples using the simple relation,

$$n_{PS} = \frac{1}{2d} \left( \frac{1}{\lambda_k} - \frac{1}{\lambda_{k+1}} \right)^{-1} \quad (1)$$

where  $d$  denotes the thickness of the porous layer, and  $\lambda_k$  is the wavelength of the  $k$ th fringe. The thickness of all porous films determined from optical microscopy measurements was about 10  $\mu$ m. The diameter of the Si nanocrystallites constituting the porous layer was estimated by Raman microspectroscopy using a method described in details elsewhere.<sup>15</sup>

#### B. Hydrogen concentration measurements

Hydrogen concentration in the fresh as-prepared PS samples was measured<sup>12</sup> by means of absorption infrared spectra of Si-H<sub>x</sub> stretching bonds obtained by an FTIR spectrometer in attenuated total reflection (ATR) measurement mode. A germanium single crystal with a refractive index of 4 was used for the infrared wave guiding and the incident beam angle was 45°. The ATR mode was chosen mainly because of the extremely small volume of the studied porous samples interacting with the testing evanescent electromagnetic field of the infrared light, in order to avoid complete loss of the detected signal due to a strong absorption from a huge number of the Si-H<sub>x</sub> bonds, as it occurs, for example, in the transmission measurement mode.

The hydrogen concentration  $N_H$  (mmol g<sup>-1</sup>) is estimated from the absorption spectra by using the following relation used earlier for an estimation of the hydrogen content in amorphous Si layers:<sup>12</sup>

$$N_H = \frac{1}{\Gamma_S \rho_{Si} (1-P)} \int_{h\nu} \frac{\alpha}{h\nu} d(h\nu) = \frac{I_S}{\Gamma_S \rho_{Si} (1-P)}, \quad (2)$$

where  $I_S$  (cm<sup>-1</sup>) is the integrated absorption of the stretching band,  $\rho_{Si}$  is the monocrystalline Si density (2.33 g cm<sup>-3</sup>),  $P$  is the porosity of the PS layer,  $\alpha$  (cm<sup>-1</sup>) is the absorption

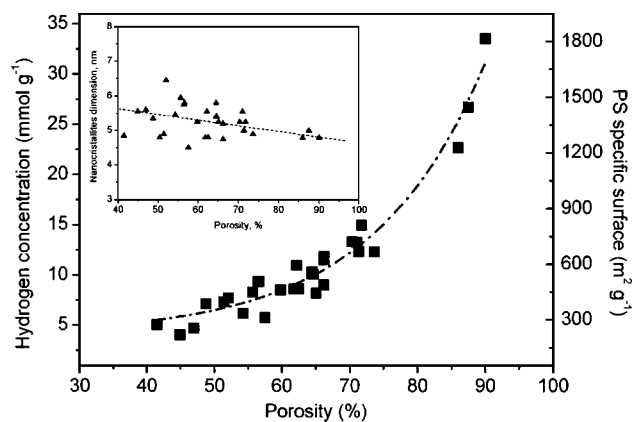


FIG. 1. Porosity-dependent hydrogen concentration in as-prepared PS and the PS estimated specific-surface area.

coefficient,  $h\nu$  is the photon energy and  $\Gamma_S(\text{cm}^2 \text{mmol}^{-1})$  is the stretching oscillator strength of the Si-H bonds (its porosity dependence is considered for our measurements) which was determined from the following relation,<sup>12</sup> as it was proposed for amorphous silicon:

$$\Gamma_S = 37.6 \times \frac{I_S}{I_W}, \quad (3)$$

where  $I_S$  and  $I_W$  are the experimentally measured integrated absorption of the stretching and wagging (near  $640 \text{ cm}^{-1}$ ) bands, respectively. Our hydrogen concentration measurements performed in the FTIR-ATR setup are found to be in excellent agreement with measurements on the hydrogen quantity thermally desorbed from the PS layer as carried out by thermally programmed desorption mass spectroscopy.<sup>12</sup>

### III. EXPERIMENTAL RESULTS

The fractal nature of the PS-specific surface can be deduced from the porosity dependence of the hydrogen concentration in the PS samples. Indeed, as it can be seen in Fig. 1, the concentration of hydrogen increases exponentially along with porosity. An excellent exponential fit of the experimental data is represented in Fig. 1 by the dash-dot line. Being bonded to the Si atoms situated at the surface of the nanocrystallites constituting the PS nanostructure,<sup>16</sup> the hydrogen concentration reflects the variation of the PS specific-surface with porosity. Taking into account that the Si atoms bonded with hydrogen atoms form mainly monohydride dimers as was recently shown by Timoshenko *et al.*,<sup>16</sup> one can estimate a mean value of the PS-specific surface assuming a mean distance (independent of crystallographic orientation) between Si atoms,  $a \approx 0.3 \text{ nm}$ . The values of the so-estimated specific surface are shown at the right axis in Fig. 1. The surface values are really huge and they take into account numerous structural crystalline defects corresponding to the Si bonds saturated by hydrogen which can penetrate far into the nanocrystallite volume. Two amazing particularities concerning the specific-surface evolution should be noted: (i) strong nonlinear enhancement with increasing porosity and (ii) larger values in comparison to those usually found for

such PS nanostructures.<sup>17</sup> Both of these facts reflect the fractal nature of the PS-specific surface.

First of all, almost constant values of the Si nanocrystallite diameters for all porosities (see inset in Fig. 1) mean that the porosity increase is mainly accompanied by structural variation of the nanocrystallites related to their surfaces. In other words, the observed total specific-surface increase along with porosity is only possible if an important fractal-like surface enhancement at a nanometer scale for each nanocrystallite is considered.

Secondly, the lower PS-specific surface values (up to  $900 \text{ m}^2 \text{ g}^{-1}$ ) in the literature are usually measured using a nitrogen adsorption technique [Brunauer-Emmett-Teller (B.E.T) method],<sup>17</sup> the molecular area (adsorption cross section) of nitrogen being taken as  $16.2 \text{ \AA}^2$ .<sup>17</sup> In our case, taking a hydrogen atom bonded to a Si atom as an elementary tile (bond cross section:  $a^2 \approx 9 \text{ \AA}^2$ ) for the specific-surface estimation, we found much larger specific-surface values (up to  $1800 \text{ m}^2 \text{ g}^{-1}$ ) and that is a typical fractal sign. Indeed, taking Mandelbrot's classic example of the coast line of Britain,<sup>18</sup> one finds that the measured length depends critically on the length of the ruler used to walk along the curve. The smaller the ruler length, the larger will be the measured length because one can follow increasingly small details (irregularities) of the curve. Similar considerations can be applied in our case in the measurement of the irregular PS-specific surface with different "tile areas," the nitrogen molecule and the Si-H bond.

The measured porosity-dependent PS-specific surface,  $S_S$ , can be well fitted by the following exponential relation:

$$S_S = A \exp\left(\frac{P}{B}\right), \quad (4)$$

where  $P(\%)$  is the porosity,  $A$  and  $B$  are the fitting parameters equal to  $37.2(\text{m}^2 \text{ g}^{-1})$  and  $23.8(\%)$ , respectively. In these terms,  $A$  is the fitting parameter representing the specific surface at  $P=0\%$ . Putting  $A=6/\rho_{Si}l_0$  according to Ref. 12, where  $\rho_{Si}=2.33(\text{g cm}^{-3})$  is the density of monocrystalline Si and  $l_0$  is the Si nanocrystallite diameter at  $P=0\%$ , we find  $l_0=69.2(\text{nm})$ . This diameter is an artificial parameter. These experimental results will be used to elaborate a fractal model describing the specific-surface morphology of the PS nanocrystallites.

### IV. FRACTAL MODEL DESCRIPTION AND DISCUSSION

Consider a single PS nanocrystallite with a fractallike surface as schematically shown in Fig. 2(a). The nanocrystallite fractal structure is modeled in the following way. The semi-spherical zero-order pits with radius,  $r_0$ ,  $k$  times smaller than the radius,  $l_0/2$ , of the initial spherical nanocrystallite,  $r_0 = l_0/2k$ , are firstly generated at two smooth semispheres of the nanocrystallite. Each large zero-order pit generates  $n$  similar first-order pits  $k$  times smaller in radius,  $r_1 = r_0/k$ , each of them producing  $n$  new once smaller second-order pits ( $r_2 = r_0/k^2$ ), and so on. Then, the radius of pits,  $r_m$ , will be:  $r_m = r_0/k^m$  and their number is  $n_m = n^m$ . Therefore, the fractal structure of the nanocrystallites is thus determined by

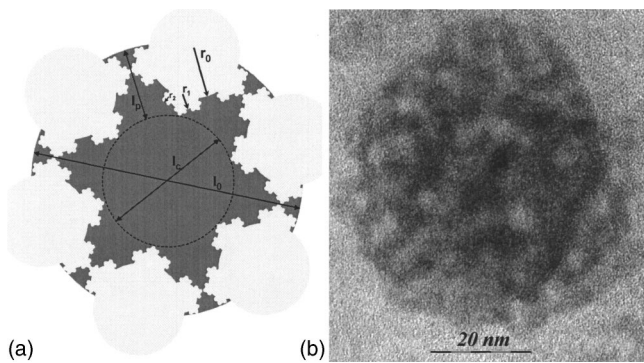


FIG. 2. (a) Schematic two-dimensional (2D) view of a single PS nanocrystallite with a fractallike specific surface.  $R_0$ ,  $r_1$ , and  $r_2$  are the radii of the zero-, first-, and second-order pits used for modeling of the fractal surface formation.  $l_0$  is the diameter of the initial nanocrystallite corresponding to  $P=0\%$ .  $l_p$  is the depth of the fractal surface penetration inside the initial nanocrystallite.  $l_c$  is the diameter of the remaining larger dimensional nanocrystallite core after the low-dimensional fractal surface formation (at  $P \neq 0\%$ ); (b) TEM image of a single PS nanocrystallite. Clear and dark regions on the image correspond to the low-order pits and to the solid Si phase, respectively.

the pair  $(k, n)$ , which is porosity-dependent and defines the fractal dimension of the pit network,  $D_p$ , as commonly accepted, by  $D_p = \ln(n)/\ln(k)$ . Such a fractal representation of the PS nanocrystallites is found to be quite close to the reality. Indeed, according to the transmission electron microscopy (TEM) image given in Fig. 2(b), a single PS nanocrystallite obtained from the grinding of a PS layer with high porosity ( $>95\%$ ) has a fractal shape which can be easily recognized. Clear and dark regions on the image correspond to the low-order pits and to the solid Si phase, respectively.

The total surface,  $S_T$ , of such a single nanocrystallite can be easily deduced,

$$S_T = S_0 \left[ 1 + \frac{1}{2} \sum_{i=1}^{m_{max}} \left( \frac{n}{k^2} \right)^i \right], \quad (5)$$

where  $S_0 = \pi l_0^2$  is the surface of the initial smooth nanocrystallite as it can be imagined at  $P=0\%$ , and  $m_{max}$  is the maximal iteration number corresponding to the smallest possible pits with radii equal to the mean distance between Si atoms ( $a=0.3$  nm as mentioned above). The integer value of  $m_{max}$  can be obtained from the following relation:  $m_{max} = [\ln(l_0/a)/\ln(k)]$  deduced from the iterative procedure of the fractal structure formation established above.

Before the calculation of the PS-specific surface,  $S_S$ , according to

$$S_S (\text{m}^2/\text{g}) = \frac{S_T}{m_{cr}}, \quad (6)$$

we calculate the mass of a single nanocrystallite,  $m_{cr}$ , which can be generally defined as

$$m_{cr} = \rho_{Si} (V_0 - V_{pits}), \quad (7)$$

where  $V_0$  and  $V_{pits}$  are the volumes of the initial nanocrystallite and that of the pits contained in it after the fractal struc-

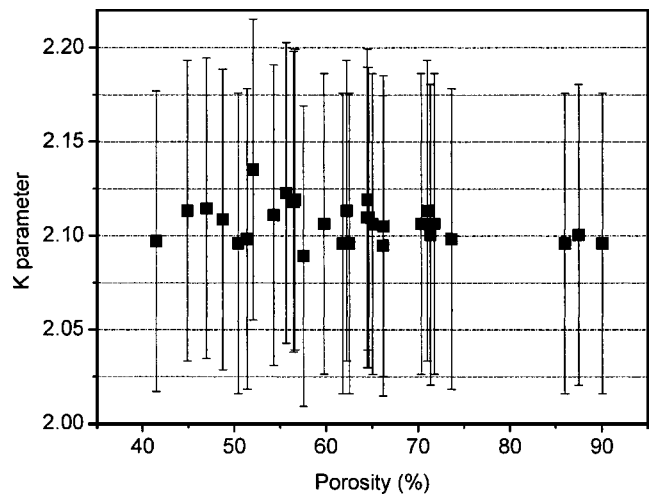


FIG. 3. Porosity dependence of the parameter  $k$  obtained using Eq. (9),  $l_c$  values (from Raman spectroscopy measurements, see the inset in Fig. 1) and  $l_0$  value (from FTIR spectroscopy measurements of hydrogen concentration, see Sec. III).

ture formation, respectively.  $V_{pits}$  can be easily determined in analogy with Eq. (5),

$$V_{pits} = V_0 \sum_{i=1}^{m_{max}} \left( \frac{n}{k^3} \right)^i, \quad (8)$$

where  $V_0 = \pi l_0^3/6$ .

To carry out numerical calculations in Eqs. (5) and (8), the values of the parameter  $k$  should be firstly determined. We obtain it using Raman spectroscopy measurements. Indeed, the nanocrystallite diameters estimated from Raman peak shift (see the inset in Fig. 1) is assumed to correspond mainly to the nanocrystallite cores with diameters of  $l_c$  as indicated in Fig. 2. Indeed, structural variations of the strongly low-dimensional fractal part of the nanocrystallite should slightly influence only the kinetics of the low-energy wing of the Raman spectra and have almost no influence on the peak position reflecting the main phonon frequency of the nanocrystallite core. Using the measured diameter  $l_c$  as a function of porosity (see the inset in Fig. 1), the value of  $l_0$  deduced from the hydrogen concentration experiments and the following estimation issued from the geometrical presentation in Fig. 2(a),

$$l_c = l_0 - 2l_p = l_0 \left[ 1 - \sum_{i=1}^{\infty} \left( \frac{1}{k} \right)^i \right] = l_0 \frac{(k-2)}{(k-1)}, \quad (9)$$

we obtain the porosity dependence of the  $k$  parameter, which is plotted in Fig. 3. This parameter is almost constant in all porosity ranges and its mean value of 2.1 is used for further calculations. Error bars take into account the uncertainty of the mean number of hydrogen atoms (0.5–2) bound to one atom of silicon that is situated at the PS surface.

Replacing parameter  $n$  in Eqs. (5) and (8) by  $n = k^{D_p}$ , where  $D_p$  is the fractal dimension of the pit network, using  $k=2.1$  as found above, and correlating Eqs. (6) and (4), the porosity dependence of  $D_p$  can be deduced. The function

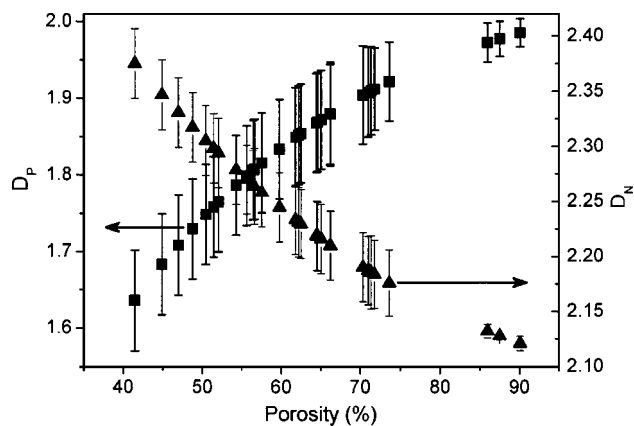


FIG. 4. Pit network ( $D_p$ , ■) and nanocrystallite ( $D_N$ , ▲) fractal dimensions as functions of the PS layer porosity.

$D_p=f(P)$  is plotted in Fig. 4. The values of  $D_p$  allow us to determine the porosity-dependent fractal dimensions,  $D_N$ , of the Si nanocrystallites constituting the PS layer. Indeed, the maximal number of pits which can completely fill the volume of the initial nanocrystallite having a diameter  $l_0$  is equal to  $k^3$ . The number of pits really used to form a given fractal structure is  $n=k^{D_p}$ . Consequently, the number of pits which could potentially fill the remaining volume of the nanocrystallite is equal to the difference,  $N=k^3-k^{D_p}$ . Thus, the fractal dimension of the nanocrystallites,  $D_N$ , determined from the classical definition,  $D_N=\ln(N)/\ln(k)$ , is also shown in Fig. 4. Similar to the case for the  $k$  parameter, the error bars in Fig. 4 take into account the uncertainty concerning the number of hydrogen atoms bound to one atom of silicon from the PS surface.

As one can see in Fig. 4, both fractal dimensions ( $D_p$  and  $D_N$ ) are strongly porosity dependent, indicating an increase of the nanocrystallites' roughness and, consequently, of the specific surface with porosity. They approach a value of 2 at porosities close to 100%, meaning that the nanocrystallites at extremely high porosities (>95%) can be represented as complex surfaces bent in space. In other words, for the high-porosity range, almost all silicon atoms are bound to hydrogen and are situated at the specific surface of the nanocrystallite. This conclusion is in excellent agreement with another simple estimation which can be done using the results of the hydrogen concentration given in Fig. 1. To illustrate this, let us analyze the sample with 90% porosity, having the highest content of atomic hydrogen (34 mmol/g). Neglecting the total mass of hydrogen in comparison with the mass of the Si skeleton, one can easily deduce that 1 g of the sample contains 36 mmol of Si atoms. Comparing these two concentration values for silicon and hydrogen atoms, we conclude that almost all Si atoms constituting the PS layer are bound with hydrogen atoms and therefore can be considered to be situated on the PS nanocrystallite surface. It means that the solid phase of the low-dimensional single PS nanocrystallite [see Fig. 2(b)] can be represented as an alloy of Si and H atoms.

The found values of  $D_N=2.1-2.4$  characterizing single nanocrystallites at subnanoscale levels and determined for a

moderate porosity range (40–70 %), are in excellent agreement with the fractal dimension values (2.36–2.47) determined by Hapko *et al.*,<sup>8</sup> who used atom force microscopy to analyze nanocrystallite arrangement at the submicroscale level onto the PS layer surface. It means that the PS nanostructure is a real fractal object with a unique fractal-dimension value for any scale level.

According to Farin and Avnir,<sup>19</sup> the hydrogen concentration  $N_H$ (mmol g<sup>-1</sup>) found at the PS-specific surface can be expressed as

$$N_H = L\sigma^{-(D_N/2)}, \quad (10)$$

where  $\sigma$  is the Si-H bond cross section ( $\approx 9 \text{ \AA}^2$ ) and  $L(\text{\AA}^{D_N} \text{ g}^{-1} \text{ mmol})$  is the lacunarity of the nanocrystallites giving additional information on their fractal texture. As pointed out by Mandelbrot,<sup>18</sup> a fractal structure with high lacunarity describes large-scale heterogeneity. In the case of our fractal model, the lacunarity values provide information on the homogeneity of pits in space and the size distribution to form the final fractal structure. The lacunarity values are especially important to compare fractal structures with close fractal dimension values (in the high-porosity range for our case). Taking into account our experimental and modeling results presented in Figs. 1 and 4, respectively, as well as Eq. (10), we obtain that (i) the general behavior of the lacunarity along with porosity is quite similar to hydrogen concentration evolution, and (ii) the lacunarity values vary from  $\approx 68(\text{\AA}^{D_N} \text{ g}^{-1} \text{ mmol})$  at low porosities to  $\approx 217(\text{\AA}^{D_N} \text{ g}^{-1} \text{ mmol})$  at high porosities, reflecting the pits' heterogeneity enhancement with increasing porosity.

## V. CONCLUSIONS

From hydrogen concentration measurements it is deduced that the specific surface of the PS nanocrystallites has a strongly fractal nature. In terms of fractal geometry, the fractal dimension of the nanocrystallites depends on the porosity of the PS nanostructures and varies in a relatively large range, 2.1–2.4. The fractal nature of the PS-specific surface should be considered in experiments for which adsorption of chemical species onto the fractal PS surface takes place. In general, this work gives a new direct proof of the fractal nature of the PS nanocrystallite morphology at nanoscale and subnanoscale levels and can be presented as additional confirmation of the analysis forwarded by M. Wesolowski in his recent paper.<sup>11</sup>

## ACKNOWLEDGMENTS

Hydrogen concentration measurements reported in this paper were performed using FTIR spectroscopy equipment of the CECOMO measurement centre from Lyon Claude Bernard University. The authors are grateful to Professor B. Champagnon and to all staff of the centre for their technical support. Dr. O. Marty from the LENaC laboratory of the Claude Bernard University of Lyon is specially acknowledged for the realization of the TEM image of a single PS nanoparticle.

- <sup>1</sup>Y. Park, *Fractals* **8**, 301 (2000).
- <sup>2</sup>O. B. Isayeva, M. V. Eliseev, A. G. Rozhnev, and N. M. Ryskin, *Solid-State Electron.* **45**, 871 (2001).
- <sup>3</sup>R. L. Smith and S. D. Collins, *J. Appl. Phys.* **71**, R1 (1992).
- <sup>4</sup>P. Goudeau, A. Naudon, G. Bomchil, and R. Herino, *J. Appl. Phys.* **66**, 625 (1989).
- <sup>5</sup>V. Vezin, P. Goudeau, A. Naudon, A. Halimaoui, and G. Bomchil, *Appl. Phys. Lett.* **60**, 2625 (1992).
- <sup>6</sup>B. J. Heuser, S. Spooner, C. J. Glinka, D. L. Gilliam, N. A. Winslow, and M. S. Boley, *Mater. Res. Soc. Symp. Proc.* **283**, 209 (1993).
- <sup>7</sup>T. F. Young, I. W. Huang, Y. L. Yang, W. C. Kuo, I. M. Jiang, T. C. Chang, and C. Y. Chang, *Appl. Surf. Sci.* **102**, 404 (1996).
- <sup>8</sup>N. Happo, M. Fujiwara, M. Iwamatsu, and K. Horii, *Jpn. J. Appl. Phys., Part 1* **37**, 3951 (1998).
- <sup>9</sup>V. M. Aroutiounian, M. Zh. Ghoolinian, and H. Tributsch, *Appl. Surf. Sci.* **162-163**, 122 (2000).
- <sup>10</sup>M. Ben-Chorin, F. Möller, F. Koch, W. Schirmacher, and M. Eberhard, *Phys. Rev. B* **51**, 2199 (1995).
- <sup>11</sup>M. Wesolowski, *Phys. Rev. B* **66**, 205207 (2002).
- <sup>12</sup>V. Lysenko, J. Vitiello, B. Remaki, D. Barbier, and V. Skryshevsky, *Appl. Surf. Sci.* **230**, 425 (2004).
- <sup>13</sup>A. Halimaoui, in *Properties of Porous Silicon*, edited by L. T. Canham (INSPEC IEE, London, 1997), p. 12.
- <sup>14</sup>D. A. G. Bruggeman, *Ann. Phys.* **24**, 636 (1935).
- <sup>15</sup>Md. N. Islam and S. Kumar, *Appl. Phys. Lett.* **78**, 715 (2001).
- <sup>16</sup>V. Yu. Timoshenko, L. A. Osminkina, A. I. Efimova, L. A. Golovan, P. K. Kashkarov, D. Kovalev, N. Künzner, E. Gross, J. Diener, and F. Koch, *Phys. Rev. B* **67**, 113405 (2003).
- <sup>17</sup>R. Herino, in *Properties of Porous Silicon*, edited by L. T. Canham (INSPEC IEE, London, 1997), p. 89; R. Herino, G. Bomchil, K. Barla, C. Bertrand, and J. L. Ginoux, *J. Electrochem. Soc.* **134**, 1994 (1987).
- <sup>18</sup>B. B. Mandelbrot, *Fractals: Form, Chance and Dimension* (Freeman, San Francisco, 1977); B. B. Mandelbrot, *The Fractal Geometry of Nature* (Freeman, San Francisco, 1982).
- <sup>19</sup>D. Farin and D. Avnir, in *The Fractal Approach to Heterogeneous Chemistry*, edited by D. Avnir (Wiley & Sons, Chichester, 1989), pp. 273–276.